A ROTATING TANK MODEL OF THE NORTH IONIAN GYRE INVERSIONS PRODUCED BY DENSE WATER FLOWS

M. Gačić (1), M. Bensi (1), V. Kovačević (1), E. Negretti (2), A. Rubino (3), J. Sommeria (2), M. Menna (1), R. Viana (3), L. Ursella (1), G. Civitarese (1), G. Siena (1), V. Cardin (1), B. Petelin (4), S. Vibaud (2), T. Valran (2)

(1) Istituto Nazionale di Oceanografia e di Geofisica Sperimentale - OGS, Italy, E-mail: mgacic@inogs.it
(2) CNRS/Grenoble-INP/UJF-Grenoble1, LEGI UMR 5519, France, E-mail: Maria-Eletta.Negretti@legi.cnrs.fr
(3) Università Ca' Foscari, Venice, Italy, E-mail: rubino@unive.it
(4) Marine Biological Station, Piran, Slovenia, E-mail: Boris.Petelin@nib.si

Results of the analysis of a rotating tank experiment simulating the response of a two-layer basin to dense-water injection are presented. The temporal evolution of the near-surface vorticity field inverts its polarity as a response to the dense water discharge, passing from weak cyclonic to strong anticyclonic. Similarities with the oceanic conditions found in the Northern Ionian Sea, which shows multiyear surface vorticity inversions are discussed. In particular, the winter 2012 situation in the Adriatic Sea, characterized by harsh meteorological conditions leading to the formation of very dense water, which was then discharged into the Ionian, is considered. In this case, the dense water of Adriatic origin caused an unusually fast inversion of the Ionian cyclonic circulation into an anticyclonic one. A comparison between the experimental results and a theoretical temporal evolution of the vorticity based on potential vorticity conservation equation shows an excellent agreement.

1. INTRODUCTION

The circulation of the upper layer of the Northern Ionian Sea is subject to periodical reversals on a decadal scale. A reversal from anticyclonic to cyclonic circulation was observed already in 1997 (Manca et al., 2003) and was associated by Borzelli et al. (2009) with the spreading of dense Cretan Sea Outflow Water (CSOW) toward the central abyssal portion of the Ionian, during the second phase of the Eastern Mediterranean Transient (EMT, Roether et al., 1996).

The available altimetric data records show that, until now, other reversals took place in 2006, 2011, and 2017, indicating that this phenomenon generally occurred every about five years, except for the post-EMT period when the cyclonic regime lasted about nine years. In the seminal paper by Gačić et al. (2010), the phenomenon of the periodical inversions of the Northern Ionian Gyre (NIG, Gačić et al., 2011) found its full explanation in terms of a complex feedback mechanism, baptized Adriatic-Ionian Bimodal Oscillating System (BiOS), which is qualitatively explained below.

Associated with the anticyclonic/cyclonic circulation mode of the NIG, less salty/saltier Atlantic Water (AW)/Levantine Intermediate Water (LIW) is advected into the Adriatic (Fig. 1). This water then contributes to shape the Adriatic winter convection, thus determining variations in density of the newly formed Adriatic Dense Water (AdDW). In the post-convection period, the AdDW spreads toward the Ionian abyss. Depending on its density, which from year to year can be larger/smaller than the ambient Ionian deep water density, it determines the horizontal pressure gradient orientation.

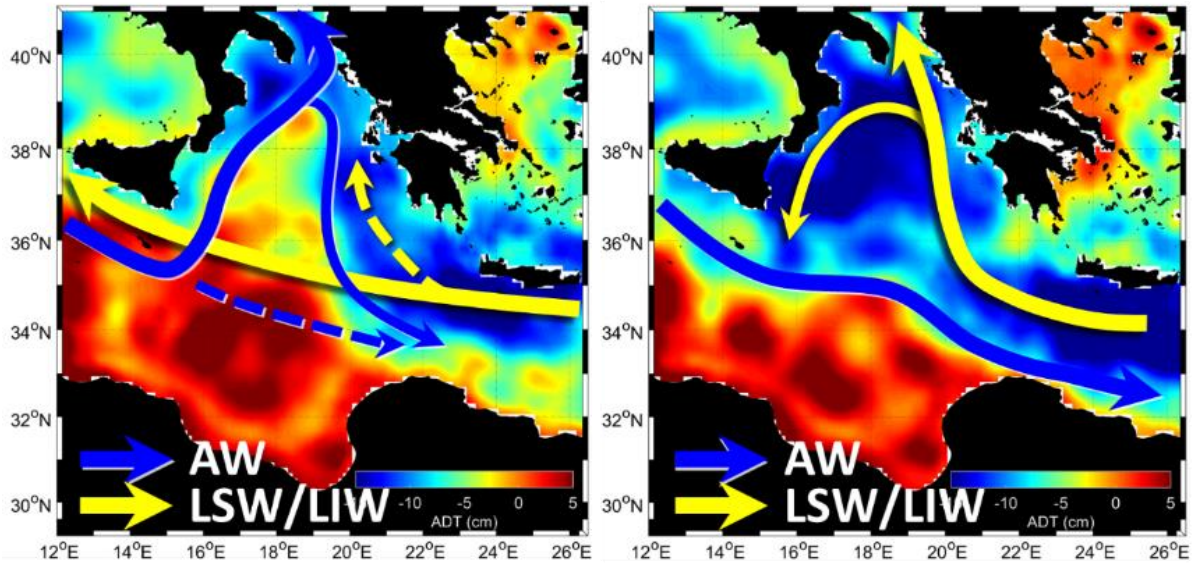

Figure 1. Schematic presentation of the flow inversions in the Ionian Sea (as from Menna et al., 2019). For the water mass acronyms see text.

During the cyclonic mode, the high-density AdDW spreads along the western continental slope in the Ionian. This results in the lowering of the sea level along the AdDW path, which creates a surface pressure gradient toward the coast and the resulting northward surface geostrophic flow. The cyclonic circulation weakens and, eventually, the anticyclonic flow takes place. Conversely, during the anticyclonic mode, relatively fresh AW enters the Adriatic causing the decrease of the AdDW density. In this situation, along the AdDW path in the Ionian (western border) the sea-level becomes higher than in the center, producing the sea surface pressure gradient responsible for the southward geostrophic flow, which eventually overwhelms the northward branch of the Ionian anticyclone creating the cyclonic basin-wide meander. In deeper layers (the layer above the vein), the northward geostrophic flow is generated due to the pressure gradient in the opposite direction. As can be seen from these considerations, the Ionian behaves as a two-layer system.

Since the Ionian interior is the crossroads of transiting Mediterranean ubiquitous waters like AW and LIW, changes in the NIG circulation pattern have also an important impact on the distribution of many oceanographic properties (Gačić et al., 2011; Gačić et al., 2014; Mihanović et al., 2015, Ozer et al., 2017). As a result, biogeochemical and biological processes occurring in the Ionian, Adriatic and Levantine seas are affected by the BiOS (Civitarese et al., 2010; Batistić et al., 2014; Vilibić et al., 2015; Ozer et al., 2017; Lavigne et al., 2018).

Due to this multifaceted impacts exerted by the NIG inversions on the marine environment, studies focusing on the BiOS mechanism, its influence and behavior, especially in the context of changes in the climatic conditions, are now flourishing.

As noted above, the cyclic inversions of the NIG show typical time scales of about five years, although sudden interruptions of the cyclonic or anticyclonic modes are possible due to particularly strong events, such as the sudden production of high-density waters in the Adriatic. Here, background conditions become the prevailing factor generating, during harsh winters, very cold high-density AdDW. This water can then invert the bottom pressure gradient in the Ionian and change the surface circulation from cyclonic to anticyclonic. Indeed, such an event was recorded in 2012 (Gačić et al., 2014) when the extremely rigid winter over the Adriatic resulted in a formation of very cold and dense AdDW. Probably not only the density of the AdDW played an important role in this inversion, but also the amount of water produced, which very likely was much larger than usual.

Generally, the BiOS-CRoPEx (Adriatic-Ionian Bimodal Oscillating System – Coriolis Rotating Platform Experiment) project was designed to broaden our understanding of the BiOS mechanism and to demonstrate the capability of internal processes to dictate the circulation in the upper thermocline.

One of the specific aims of the BiOS-CRoPEx project was to try to simulate the 2012 situation, when exceptionally dense AdDW outflow in spring 2012 inverted temporarily the NIG circulation pattern. In this paper, we will compare the *in situ* oceanographic and experimental data, and discuss differences and similarities between the physical model and the real ocean. This exercise will give us the opportunity to study in more details the mechanism responsible for the circulation inversions and the impact of climatic conditions on the cyclical variations of the circulation in the Ionian Sea.

2. EXPERIMENTAL DESIGN, MEASUREMENT TECHNIQUES AND DATA ANALYSIS

Experiments were conducted at the Coriolis rotating platform at LEGI, in a circular tank of 13 m diameter and 1 m depth. The experimental setup is shown in Figure 2. The slope was realized using an axisymmetric conical-shaped boundary descending toward the center of the tank with a slope s of 0.1. The total width of the slope was 4 m. It gradually descended from the tank edge, where its height was 40 cm, down to the tank bottom. Hence, the central (deep) portion of the tank with constant depth had a diameter of 5 m.

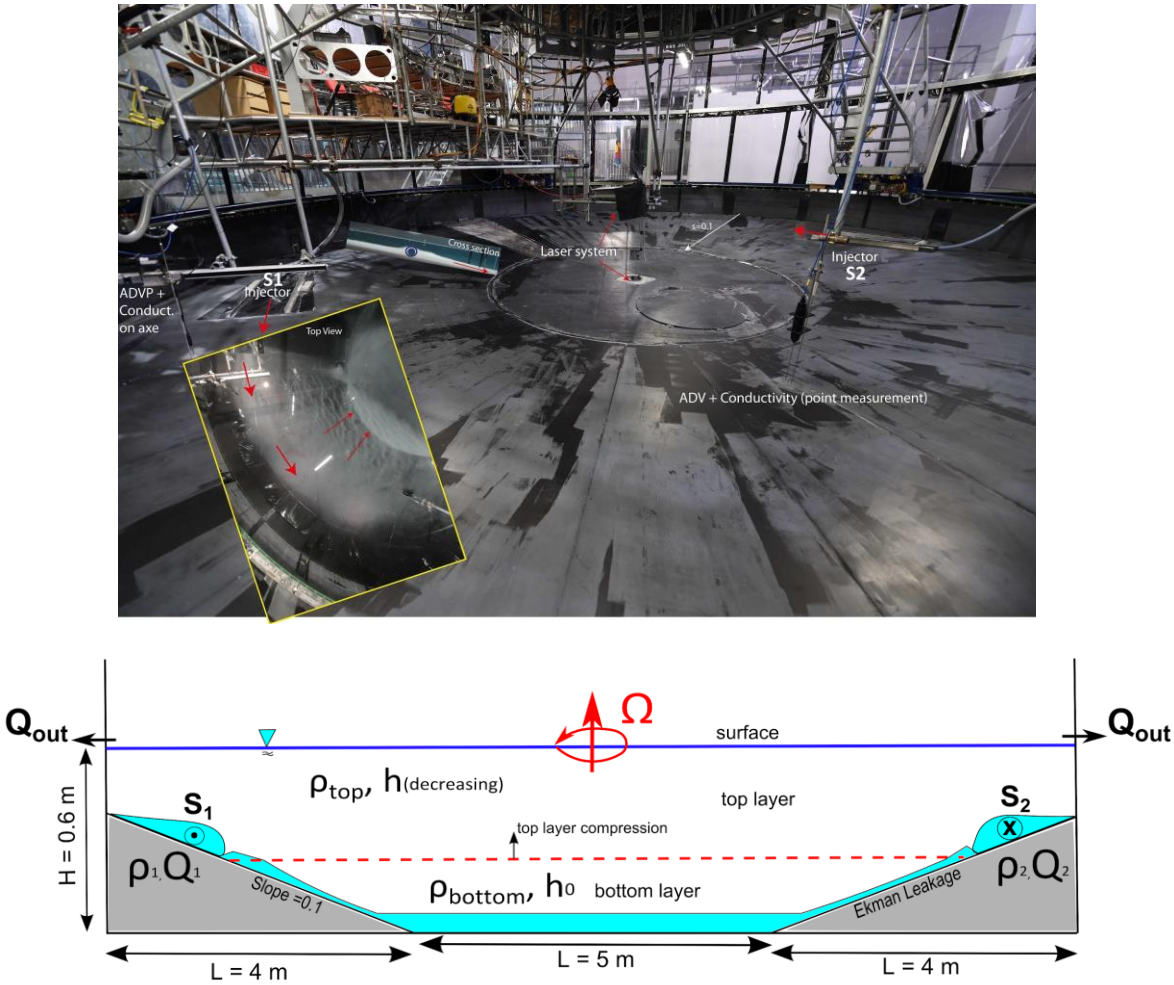

Figure 2. Experimental setup (two-layer system).

The tank, put on constant anticlockwise (cyclonic) rotation, was initially filled with two layers of different densities. The filling lasted several hours, in order to assure a minimum interface thickness and reach a solid-body rotation. Saline solutions were injected through specifically designed devices, which consisted of a tube ending on a rigid plate and a flexible plastic cover, fixed at the two sides to the bottom plate, 50 cm wide and 2 m long. This configuration enables the saline current to adjust geostrophically within the tube without mixing with the fresh ambient water during the adjustment

phase. The flow rate Q and dimensions of the injector (L, h_j) were estimated prior to the experiment. The scope was to obtain velocities of the order of the Nof speed u = g' s/f (a theoretical along-slope speed of a geostrophically balanced dense water fluid; Nof, 1983), where f = 4π/T, T is the rotation period, s is the slope, and Q = uh_jL. With this balance, the injection systems S1 and S2 positioned 1 m from the top of the slope area, generated a density current in the direction of rotation 50 cm wide (L) and maximum 2 cm high (h_j) at the device outlet (Fig. 2). The flow rate, ranging between 0.4 and 1.6 l s^{-1}, was controlled by a pump with a maximum capacity of 4 l s^{-1}. Outlets were opened beyond the conical slope at the tank bottom to keep the total water depth constant throughout the experiment duration and allow discharging the fresh water by the thin gap around the upper circular end of the slope, assuring also the minimal disturbance to the flow in the central part of the tank.

Polyamide particles (Orgasol) with a mean diameter of 60 μm and a density of 1.016 g cm^{-3} were added to both the salt and the fresh water layers and to the injected saline solutions as tracers for velocity measurements with particle image velocimetry (PIV). A 25 W Yag laser operating with wavelength λ = 514 nm was used as a continuous light source. The beam was transmitted through different mirrors within a glass cylinder with a diameter of 30 cm in the center of the tank where a rotating mirror optical system generated a horizontal laser sheet of 130 m^2 and a thickness of roughly 5 mm. The systems moved vertically through a Labview controlled linear axis to permit a scan of the depth with 12 different levels equidistant by 4 cm, the highest and lowest levels being at 51 cm and 7 cm from the bottom, respectively. Images of 13 m × 9 m were taken with a Nikon Camera (D850 SLR, 45MPx) at a frame rate of 1 Hz, synchronized with the laser system. With the use of an optical lens of 14 mm on the camera, the spatial resolution was 1 mm $pixel^{-1}$. With the software UVMAT developed at LEGI, the velocity fields were computed using a cross-correlation PIV algorithm. For this purpose, an adaptive multi-pass routine was used, starting with an interrogation window of 35×35 pixels and a final window size of 20×20 pixels, with 70 % overlap. Each vector of the resulting vector field represented an area of roughly 0.5×0.5 cm. The velocity vectors were post-processed using a local median filter. Given the velocities encountered in the experiments, the experimental error in the instantaneous velocity was estimated to be approximately 3% and in $\partial u/\partial x$ approximately 10% maximum.

The velocity and the density at the outlet were monitored by means of an Acoustic Doppler Velocimetry Profiler (ADVP, Vectrino) and a conductivity probe. Both instruments were mounted 1 m downstream of the injector outlet S1 on a traversing system that enabled continuous periodic measurements on a radial section of 1 m length. Three velocity components were measured in a vertical section within the layer 3.5 cm wide and parallel to the bottom slope, while the density was calculated from conductivity values recorded at a distance of 1 cm from the bottom. An additional acoustic Doppler velocimeter (Vectrino) and a conductivity probe, mounted 4 m downstream of the injector outlet S1, were used to capture velocities and densities 1 cm from the bottom. A conductivity probe was positioned in the central (deep) part of the tank and mounted on a third traverse system enabling to take continuously vertical density profiles during the experiments.

The initial condition for the chosen experiment was a two-layer system, with ρ_{top} = 999.5 kg m^{-3}, ρ_{bottom} = 1014.7 kg m^{-3} and respective heights h_{top} = 21 cm and h_0 = 36 cm. The rotation period T was set to 120 s. Two sources of saline injections were used, the first, S1, injecting ρ_1 = 1010 kg m^{-3} at a rather low flow rate of 0.4 ls^{-1} from the beginning of the experiment, the second, S2, positioned 180 degrees downstream from the first outlet with ρ_2 = 1019.8 kg m^{-3} at a flow rate of 1.6 ls^{-1}. The second source was switched on 90 minutes (45 experimental "days", i.e. rotation periods) after the beginning of the experiment. It was then switched off after 180 minutes, when the flow rate of the S1 source was doubled to 0.8 l s^{-1}. Discharge from S1 continued for 60 minutes more. In total, the experiment lasted 270 minutes (i.e., 135 "days").

The altimetric data used for the study of the evolution of the Ionian surface circulation were the gridded (1/8° Mercator projection grid), daily Absolute Dynamic Topography (ADT) and the corresponding Absolute Geostrophic Velocities (AGV) distributed by CMEMS-Copernicus Marine Environment Monitoring Service (SEALEVEL_MED_PHY_L4_REP_OBSERVATIONS_008_051). Vorticity was averaged over the rectangular area of the Northern Ionian (37-39 °N, 17-19 °E) and normalized by a Coriolis parameter (10^{-4} s^{-1}). Similarly, the vorticity from the PIV measurements was normalized by the Coriolis parameter of the tank (10^{-1} s^{-1} – 120 s rotational period) and averaged within the plain deep central area.

3. PREDICTIONS OF MEAN CIRCULATION AND TIME SCALES

In order to show that internal processes, compressing the upper freshwater layer, induce the circulation in the upper layer, we consider the equation of conservation of potential vorticity, with ζ representing the relative vorticity, h is a time dependent depth of the bottom layer. The variation in depth $\partial h/\partial t$ is related to the injected flow rate as: $\partial h/\partial t = Q/(\pi R(t)^2)$, where $R(t)=R_0+h(t)/s$ being the radius of the interfacial layer which depends on time t, s is a slope and R_0 is the radius of the central (deep) region. This gives thus

$$\frac{\partial \zeta}{\partial t} = \frac{f}{h}\frac{\partial h}{\partial t} = \frac{f}{h}\frac{Q}{\pi(R0+h/s)\text{^}2}.$$

Figure 3c shows the variation of the vorticity, spatially averaged within the central region (with a radius of 2.5 m), whereas different colors indicate the various horizontal layers in the vertical. The start of the injection of deep salty water (the S2 source) is highlighted at t/T=45 and cessation at t/T=90. We see that once the dense water source is switched on, the circulation in the upper layer quickly changes sign, from slightly cyclonic (due to weak residual motions in the tank) to anticyclonic shortly after t/T=45. The vorticity reaches a minimum value around -0.0175 s^{-1}, roughly in correspondence with the switching off the second source. Monotonous decrease of the anticyclonic vorticity then takes place until the end of the experiment. We believe that the reversal to the cyclonic vorticity was not observed due to the relatively short experiment duration. The vorticity in the deepest layers was close to zero during the entire experiment duration except for the period immediately after the beginning of the dense water injection when the clear cyclonic vorticity appeared. We compared the experimental results with the theoretical prediction of the vorticity variations in time as given in the equation of the potential vorticity conservation, obtaining an excellent agreement.

4. RESULTS AND DISCUSSION

Surface circulation was weakly cyclonic before the injection of the dense water (ρ_2) due to a residual initial flow (Fig. 3a). After the injection of the dense water, the surface circulation turned into the rather strong and persistent anticyclonic flow (Fig. 3b). At the beginning of the dense water injection, the vorticity in the bottom layer (Fig. 3c) was slightly positive, but of smaller absolute values than the surface anticyclonic vorticity. It is important to notice that, generally, the anticyclonic vorticity was stronger than the cyclonic one, i.e., the systems shows a preference for the water column to rotate anticyclonically. This result differs from previous studies, which are however related to processes characterized by large Rossby numbers (≥ 1, see Rudnyck, 2001), and show a preference for cyclonic circulation. In our experiment, instead, the Rossby number was O(0.1).

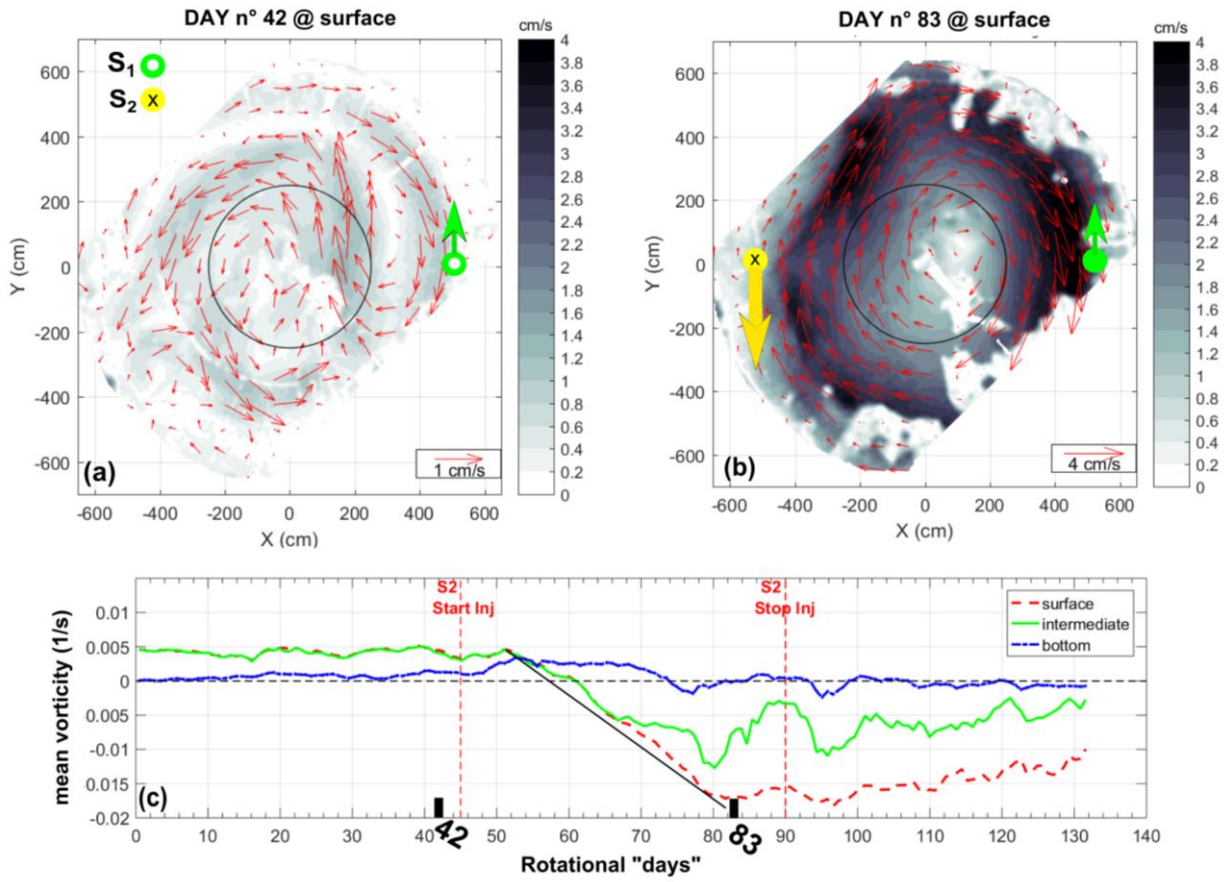

Figure 3. Horizontal distribution of the flow and vorticity field in the uppermost level at “rotational day” 42, before S2 source injection (a) and at “day” 83 (b). Panel c shows the time evolution of the spatially averaged vorticity within the deep portion of the tank in three layers: surface (including levels 2-4), intermediate (level 7) and bottom (including levels 10-12). The black solid line represents the theoretical prediction of vorticity variations using equations of the potential vorticity conservation.

The vorticity evolution in the upper layer of the rotating tank (Fig. 3) shows quite a quick response of the vorticity field to the dense water injections (day 45); after about ten days (day 55) there is a sudden switch to anticyclonic vorticity with its progressive intensification. Finally, the curve flattens out after about another twenty days (day 80). The intermediate level (close to the interface) shows anticyclonic vorticity as well. However, it is less intense than for the upper layers and fluctuates in such a way that minimum values occur about every ten days. This behavior corresponds to the passage of cyclonic eddies through the central plain area. The mesoscale cyclones are evident at almost all levels (not shown) with the largest amplitude at the interface, between days 80 and 100, which suggests that they might be subsurface intensified structures. The horizontal distribution of the flow field (not shown) indeed confirms the formation or the passage of these subsurface intensified cyclones. The temporal evolution of the bottom layer vorticity reveals an increase of the cyclonic vorticity from the beginning of the dense water injection, which reduces to zero rather soon (Fig. 3c).

Winter 2012, which was characterized by the formation of an extremely dense water in the Adriatic, resulted, during spring 2012, in a spreading of this newly formed water into the Ionian, which caused a transient inversion of the Ionian cyclonic circulation (Gačić et al., 2014). This physical situation should be similar to the analyzed experiment in the rotating tank. In the paper of Gačić et al. (2014), the start of the very dense AdDW discharge into the Ionian was determined with rather satisfactory precision and we are thus able to compare the evolution of the *in situ* vorticity and the rotating tank vorticity, starting from the moment of the dense water injection (Fig. 4). The *in situ* geostrophic flow is determined from altimetric data and thus the associated surface vorticity field represents the geostrophic vorticity; therefore, the two vorticity fields are not fully comparable.

However, as in the case of the rotating tank, the response of the Ionian near-surface geostrophic vorticity field was quite fast (on the order of a month); differences appeared instead in the time needed to reach the quasi-steady state, which in the Ionian is about two times longer than in the rotating tank. Differences in the response time between the rotating tank experiment and the Ionian Sea case can be estimated from the non-dimensional number, i.e. the ratio between the inertial period and the residence time, which we show to be almost twice as large in the real ocean than for the tank experiment.

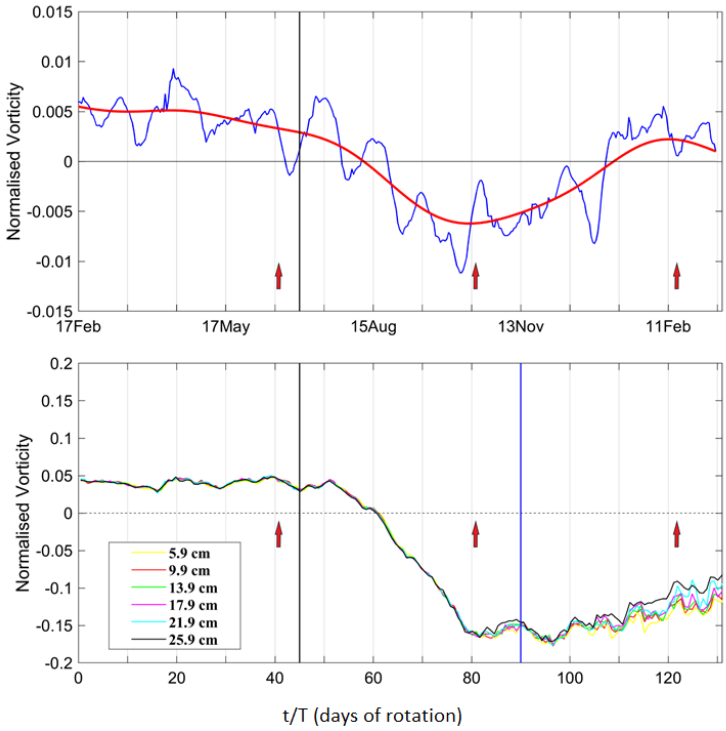

Figure 4. Normalized vorticity for the Northern Ionian Sea (a) and for the tank experiment (b). Red arrows indicate the elapsed times corresponding to the histograms shown in Fig. 5.

The histograms of vorticity distribution (Fig. 5) at all levels show, generally, a shape close to the Gaussian distribution. The histograms for the surface layer reveal clearly the evolution of the flow field before and after the start of the dense water discharge. Vorticity inverts into the anticyclonic mode after the 45th day of the experiment. After the dense water injection ceases, a secondary maximum occurs at positive vorticity values. The asymmetry is also evident at the density interface where during the injection period two peaks occur: one in the anticyclonic and one in the cyclonic part. As expected, the vorticity histogram for the interface deviates largely from the Gaussian distribution (Fig. 5e) during the dense water discharge due to heterogeneous velocity field and the presence of both cyclonic and anticyclonic mesoscale structures. After ceasing of the S2 dense water injection, while the S1 light water injection continues, there is a slow decrease of the absolute values of the anticyclonic vorticity in the surface layer. Indeed, on the 123th day a secondary weak maximum at positive (cyclonic) vorticity values shows up. However, a complete reversal could not have been reached, due to a relatively short experiment duration after the cessation of the dense water injection.

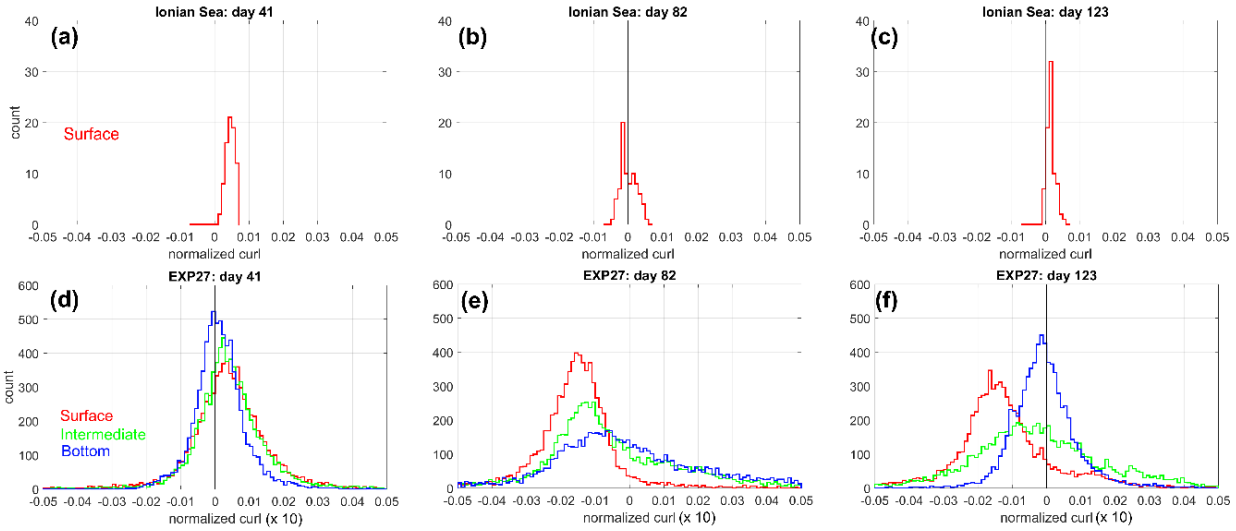

Figure 5. Histograms of the mean normalized vorticity in three different moments: before, after and during dense water injection. Upper panels (a, b, c) refer to the surface layer in the Ionian Sea, while lower panels (d, e, f) refer to the central part of the rotating tank at three measurement levels (surface level 1, intermediate level 7, and bottom level 12). The days in the upper panels indicate time scaled by a factor 0.5 (see text) in order to obtain the same slope of both Ionian and tank vorticity curves.

We discuss the *in situ* vorticity distribution at the same days when we choose the rotating tank vorticity distribution. However, in order to have similar physical conditions in both data sets we had to rescale the time axis of the *in situ* data by multiplying the time interval of the Ionian Sea vorticity evolution by a factor of 0.5, as seen above. We have also to consider that before the start of the AdDW injection into the Ionian, the background *in situ* conditions were characterized by a cyclonic circulation, different from the case in the rotating tank. In fact, on the 41st day a peak of the vorticity histogram is at the positive vorticity value and then on the 82nd day (during the AdDW discharge) the peak moves toward negative values, showing anticyclonic circulation. The histogram of the 88th day is highly asymmetric, with the maximum at anticyclonic vorticity values (not shown). On the 123rd day the peak returns back to a positive vorticity value meaning that the impact of the AdDW weakened appreciably and the system went back to the initial cyclonic circulation.

5. CONCLUSIONS

In this paper, we discuss results of the analysis of an experiment, which was conducted at the Coriolis rotating platform at LEGI in the framework of the CroPEx project. The experiment consisted of three phases; in the first phase, relatively light water (1015 kg m^{-3}) was injected for about one-third of the experiment duration into the two-layer system. Then, a second source was added and very dense water (1020 kg m^{-3}, denser than the deep-layer density) was injected for 45 rotations (days) and, finally, after the cessation of the dense water injection, the light water continued discharging for about 50 days at a double discharge rate with respect to its initial injection rate. The experiment was thought to be dynamically similar to the situation occurred in the Ionian basin after winter 2012. Climatic conditions in the area were characterized by an extremely harsh winter over the region and, consequently, the Adriatic Sea produced very dense water, which was then discharged into the Ionian Sea and was able to invert temporarily the Ionian circulation from cyclonic to the anticyclonic one.

The evolution of the vorticity field in the rotating platform shows strong similarities with the *in situ* situation; quite a sudden inversion of the surface circulation from the cyclonic to the anticyclonic took place both in the Ionian Sea and in the rotating platform after the dense water injection. However, differences in the response time scale are evident and the response is almost twice as fast in the physical experiment than in the Ionian. This relationship between the response time in the Ionian and in the rotating tank is obtained from a non-dimensional number, i.e. the ratio between the inertial period and the residence time of the receiving basin (the Ionian Sea or the central plain area of the rotating tank). It can be shown that the response time is larger for the tank experiment than for the Ionian Sea.

Starting from the equation of conservation of potential vorticity, we showed quite a good agreement between the experimental data and theoretical estimates of the rate of change of the vorticity. After about 20 (rescaled) days from the beginning of the dense water discharge, the anticyclonic vorticity reaches a plateau in both the real ocean and in the rotating tank. From the field observations, it can be seen that the flow after some time returns to the cyclonic mode when probably the Adriatic dense water impact weakens. In the rotating tank, after the cessation of the dense water injection, the anticyclonic vorticity started to weaken but did not come back to the cyclonic flow probably due to the relatively short duration of the experiment. With this experiment and comparison with *in situ* data, we thus show how climatic conditions responsible for a sudden increase of the bottom water density in the Adriatic can change the "internally" dictated rhythm of the circulation inversions in the Ionian Sea, definitely confirming the robustness of the BiOS mechanism.

ACKNOWLEDGMENTS

This project has received funding from the European Union's Horizon 2020 research and innovation program under grant agreement No 654110, HYDRALAB+. We express our thanks to P. Del Negro, Director of the Istituto Nazionale di Oceanografia e di Geofisica Sperimentale - OGS, Trieste for her continuous encouragement and great interest for our project during the preparatory work and its realization. We appreciated very much the collaboration with the LEGI staff in the preparatory, realization and post-processing phases of the experiment.

REFERENCES

Batistić M., Garić, R., Molinero J.C. (2014). Interannual variations in Adriatic Sea zooplankton mirror shifts in circulation regimes in the Ionian Sea. Clim. Res., Vol. 61: 231–240, doi: 10.3354/cr01248.

Borzelli, G. L. E., Gačić, M., Cardin, V. and Civitarese, G. (2009). Eastern Mediterranean Transient and reversal of the Ionian Sea circulation, Geophys. Res. Lett., 36, L15108, doi:10.1029/2009GL039261.

Civitarese, G., Gačić, M. Lipizer, M. and Eusebi Borzelli, G. L. (2010). On the impact of the Bimodal Oscillating System (BiOS) on the biogeochemistry and biology of the Adriatic and Ionian Seas (Eastern Mediterranean), Biogeosciences, 7, 3987–3997, doi:10.5194/bg-7-3987-2010.

Gačić, M., Eusebi Borzelli, G.L. Civitarese, G. Cardin V. and Yari, S. (2010). Can internal processes sustain reversals of the ocean upper circulation? The Ionian Sea example, Geophys. Res. Lett., 37, 10 L09608, doi:10.1029/2010GL043216.

Gačić, M., Civitarese, G., Kovačević, V., Poulain, P-M., Theocharis, A., Menna, M., Catucci, A., Zarokanellos, N. (2011). On the relationship between the decadal oscillations of the Northern Ionian Sea and the salinity distributions in the Eastern Mediterranean. J. Geoph. Res.; 116. C12002, doi:10.1029/2011JC007280.

Gačić, M., Civitarese, G., Kovačević, V., Ursella, L., Bensi, M., Menna, M., Cardin, V., Poulain, P.-M., Cosoli, S., Notarstefano, G., and Pizzi, C. (2014). Extreme winter 2012 in the Adriatic: an example of climatic effect on the BiOS rhythm, Ocean Sci., 10, 513-522, https://doi.org/10.5194/os-10-513-2014.

Lavigne, H., Civitarese, G., Gačić, M., and D'Ortenzio, F. (2018). Impact of decadal reversals of the north Ionian circulation on phytoplankton phenology, Biogeosciences, 15, 4431-4445, https://doi.org/10.5194/bg-15-4431-2018.

Manca, B.B., Budillon, G. Scarazzato, P. and Ursella, L. (2003). Evolution of dynamics in the eastern Mediterranean affecting water mass structures and properties in the Ionian and Adriatic seas, J. Geophys. Res., 108(C9), 8102, doi:10.1029/2002JC001664..

Menna, M., Reyes Suarez, N.C., Civitarese, G., Gačić, M., Rubino, A., Poulain, P.-M. (2019). Decadal variations of circulation in the Central Mediterranean and its interactions with mesoscale gyres. Deep Sea Res. II, 2019, doi:10.1016/dsr2.2019.02.004.

Mihanović, H., Vilibić, I., Dunić, N. and Šepić, J. (2015). Mapping of decadal middle Adriatic oceanographic variability and its relation to the BiOS regime, J. Geophys. Res. Oceans, 120, 5615–5630, doi:10.1002/5JC010725.

Nof, D. (1983). The translation of isolated cold eddies on a sloping bottom. Deep-Sea Res. **30**, 171–182.

Ozer, T., Gertman, I., Kress, N., Silverman, J., and Herut, B. (2017). Interannual thermohaline (1979–2014) and nutrient (2002–2014) dynamics in the Levantine surface and intermediate water masses, SE Mediterranean Sea. Global and Planetary Change 151, 60–67.

Roether, W., Manca, B.B., Klein, B., Bregant, D., Georgopoulos, D., Beitzel, V., Kovačević, V., and Luchetta, A. (1996). Recent Changes in Eastern Mediterranean Deep Waters. Science, 271, 333-335.

Rudnyck, D.L. (2001). On the skewness of vorticity in the upper ocean. Geophys. Res. Lett., Vol. 28, 10, 2045-2048, https://doi.org/10.1029/2000GL012265

Vilibić I., Mihanović H., Kušpilić G., Ivčević A., and Milun, V. (2015). Mapping of oceanographic properties along a middle Adriatic transect using Self-Organising Maps, Estuarine, Coastal and Shelf Science, 163, 84-92.